2018

Tissue specific differences in mitochondrial DNA maintenance and expression

Herbers, Elena

Elsevier BV

Tieteelliset aikakauslehtiartikkelit

http://dx.doi.org/10.1016/j.mito.2018.01.004

Tissue specific differences in mitochondrial DNA maintenance and expression

Elena Herbers, Nina J. Kekäläinen, Anu Hangas, Jaakko L. Pohjoismäki, Steffi Goffart

PII: S1567-7249(17)30342-2
DOI: doi:10.1016/j.mito.2018.01.004
Reference: MITOCH 1260

To appear in: *Mitochondrion*

Received date: 18 December 2017
Revised date: 5 January 2018
Accepted date: 11 January 2018

Please cite this article as: Elena Herbers, Nina J. Kekäläinen, Anu Hangas, Jaakko L. Pohjoismäki, Steffi Goffart , Tissue specific differences in mitochondrial DNA maintenance and expression. The address for the corresponding author was captured as affiliation for all authors. Please check if appropriate. Mitoch(2018), doi:10.1016/j.mito.2018.01.004

Tissue specific differences in mitochondrial DNA maintenance and expression

Elena Herbers, Nina J. Kekäläinen, Anu Hangas, Jaakko L. Pohjoismäki & Steffi Goffart

Department of Environmental and Biological Sciences, University of Eastern Finland, P.O. Box 111, FI-80101, Joensuu, Finland.

Abstract

The different cell types of multicellular organisms have specialized physiological requirements, affecting also their mitochondrial energy production and metabolism. The genome of mitochondria is essential for mitochondrial oxidative phosphorylation (OXHPOS) and thus plays a central role in many human mitochondrial pathologies. Disorders affecting mitochondrial DNA (mtDNA) maintenance are typically resulting in a tissue-specific pattern of mtDNA deletions and rearrangements. Despite this role in disease as well as a biomarker of mitochondrial biogenesis, the tissue-specific parameters of mitochondrial DNA maintenance have been virtually unexplored.

In the presented study, we investigated mtDNA replication, topology, gene expression and damage in six different tissues of adult mice and sought to correlate these with the levels of known protein factors involved in mtDNA replication and transcription. Our results show that while liver and kidney cells replicate their mtDNA using the asynchronous mechanism known from cultured cells, tissues with high OXPHOS activity, such as heart, brain, skeletal muscle and brown fat, employ a strand-coupled replication mode, combined with increased levels of recombination. The strand-coupled replication mode correlated also with mtDNA damage levels, indicating that the replication mechanism represents a tissue-specific strategy to deal with intrinsic oxidative stress. While the preferred replication mode did not correlate with mtDNA transcription or the levels of most known mtDNA maintenance proteins, mtSSB was most abundant in tissues using strand-asynchronous mechanism. Although mitochondrial transcripts were most abundant in tissues with high metabolic rate, the mtDNA copy number per tissue mass was remarkably similar in all tissues. We propose that the tissue-specific features of mtDNA maintenance are primarily driven by the intrinsic reactive oxygen species exposure, mediated by DNA repair factors, whose identity remains to be elucidated.

Keywords: mitochondrial DNA, mtDNA replication, mtDNA maintenance, mtDNA recombination

1. Introduction

Mitochondria are essential organelles producing most of the cellular ATP by means of oxidative phosphorylation (OXPHOS) and are present in every cell type except red blood cells. Mammalian tissues differ in many respects in their metabolic profiles as well as energy demands and these parameters can change during development, physiological adaptation and pathology (Alston et al., 2017; Jayashankar et al., 2016; Johnson et al., 2007a; Kunz, 2003; Pohjoismaki and Goffart, 2017; Schrepfer and Scorrano, 2016). It is therefore not surprising that the cardiomyocyte mitochondria, specialized in constant and effective production of ATP by the means of β-oxidation, are inherently different from mitochondria in liver and kidney cells, more specialized for various reactions of anabolic and catabolic metabolism. The difference is not only restricted to gene expression and mitochondria protein composition (Johnson et al., 2007b), but also OXPHOS function (Fernandez-Vizarra et al., 2011) and mitochondrial DNA maintenance (Pohjoismaki and Goffart, 2011). These tissue-specific requirements as well as their specialized mitochondrial features are quite likely the reason why some tissues are more affected than others in mitochondrial disorders (Alston et al., 2017).

Mitochondria have their own small circular genome, mtDNA, which encodes for the 13 essential subunits of the electron transport chain and ATP synthase together with 22 tRNAs and two rRNAs required for mitochondrial protein synthesis. Mitochondrial DNA copy number varies depending on the cell type and its maintenance as well as gene expression are controlled by nuclear-encoded factors (Falkenberg et al., 2007). One of the most important maintenance proteins is the mitochondrial transcription factor A, or TFAM, whose levels closely correlate with mtDNA copy number, regardless of the cell type (Kukat et al., 2015; Pohjoismaki et al., 2013a). According to the current understanding, TFAM is mainly a

structural protein of the mitochondrial nucleoid, involved in packing mtDNA and enabling its transcriptional regulation by other factors such as mitochondrial transcription factor B2 (TFB2M) (Fukuoh et al., 2009; Kanki et al., 2004; Kukat et al., 2015; Rubio-Cosials et al., 2011; Shi et al., 2012). Loss of TFAM results in the depletion of mtDNA, probably due to increased turnover as well as lack of replication initiation (Ekstrand et al., 2004; Pohjoismaki et al., 2006), making it a prime candidate responsible for the regulation of mtDNA copy number (Matsushima et al., 2010). Both TFAM and TFB2M are controlled by nuclear respiration factor 1 (NRF-1), one of the key regulators of mitochondrial biogenesis (Scarpulla, 2008). While variations in mtDNA copy number were long thought to be responsible for the differences in mitochondrial protein expression, recent evidence points that mtDNA might have merely a housekeeping function, as its levels are kept rather constant per tissue mass during heart development (Pohjoismaki et al., 2012; Pohjoismaki et al., 2013a). Instead, much of the increase in OXPHOS activity can be attributed to increased rate of mtDNA expression by TFB2M (Pohjoismaki et al., 2012). As TFB2M is known to be required for the recruitment and promoter specificity of mitochondrial RNA polymerase (POLRMT) (Shi et al., 2012), it is likely that the regulation of mitochondrial gene expression by rapidly adjustable protein factors is much more important than fine-tuning the gene copy number.

Animal mitochondria do not have a replicative primase enzyme, instead POLRMT is quite likely generating primers for mtDNA replication (Fuste et al., 2010; Pham et al., 2006; Torregrosa-Munumer et al., 2017). These primers are elongated by the mitochondrial DNA polymerase γ, consisting of one catalytic subunit (Pol γA) and two accessory subunits (Pol γB).Pol γB essential for the enzyme activity as it can stimulate DNA synthesis 100-fold by enhancing DNA and nucleotide binding (Ciesielski et al., 2016). The rate-limiting factor for

mtDNA replication is the mitochondrial helicase TWNK (or PEO1) (Goffart et al., 2009; Tyynismaa et al., 2004; Wanrooij et al., 2007), required for the unwinding of the DNA helix at the replication fork. Together with mitochondrial single-strand binding protein (mtSSB), these factors constitute the only known members of the mitochondrial replisome (Korhonen et al., 2004). TWNK has also recombinase activity *in vitro* (Sen et al., 2012; Sen et al., 2016) and its transgenic overexpression in mouse increases mtDNA recombination (Pohjoismaki et al., 2009; Pohjoismaki et al., 2013b), making it a prime candidate for the elusive mitochondrial recombinase in animals. Abundant recombination intermediates have otherwise been only observed in human heart and brain (Pohjoismaki et al., 2009) as well as mouse heart (Goffart et al., 2009). Circumstantial evidence suggests that recombination might have a protective role against mtDNA damage in highly oxidative tissues (Pohjoismaki et al., 2013b). There are also tissue specific differences in mtDNA replication intermediates. While most tissues and cultured cells replicate their mtDNA in highly asynchronous manner, with lagging-strand synthetized with considerable delay (Miralles Fuste et al., 2014; Reyes et al., 2013), the replication intermediates of skeletal muscle, heart and brain are typical for more conventional strand-coupled replication (Goffart et al., 2009; Pohjoismaki et al., 2009). The biological significance as well as the regulation of the two different replication mechanisms remains unknown.

Mitochondrial DNA has various topological forms, including supercoils, catenanes and unicircular dimers (Kolesar et al., 2013). In addition, the non-coding region of the mtDNA often contains a curious structural feature, the displacement loop (D-loop), where 650 bp long single-stranded 7S DNA is hybridized on double-stranded DNA to form triple-stranded structure. The purpose of the D-loop is unknown, but the 7S is thought to be generated by premature replication termination at TAS sequence shortly downstream of the main

replication origin O_H (Crews et al., 1979; Fish et al., 2004). Interestingly, much of the 7S within mitochondria is unbound and requires mtSSB for stability (Ruhanen et al., 2010).

In the presented study, we aimed to address the tissue specific differences in mitochondrial DNA maintenance, comparing mtDNA levels and integrity and see if these features correlate with mtDNA replication mode, ratio of replication factors and the level of mitochondrial gene expression. We found mitochondrial gene expression to be highest in heart and brown adipose tissue, known to have a high oxidative metabolism. Interestingly, neither mtDNA copy number nor abundance of transcription machinery factors correlated with the levels of mitochondrial transcripts.

The investigated tissues showed striking differences in the way mitochondrial DNA is replicated: the tissues expected to have active mitochondrial respiration, such as heart, skeletal muscle, brain and brown fat, showed higher levels of mtDNA damage and at the same time contained mtDNA molecules with four-way junctions typical for DNA recombination. This damage was correlating with strand-coupled replication and signs of recombination, suggesting that mtDNA recombination might be a way of repairing oxidative damage. In contrast, liver and kidney mtDNA having less damage replicate via the strand-asynchronous replication mode known from cultured cells, and fittingly they possess higher levels of the mitochondrial single-stranded binding protein SSB1. Our results indicate that the mode of mtDNA replication correlates with the damage that mtDNA is susceptible to, suggesting the observed differences in mitochondrial DNA replication to be an adaptation to varying levels of genotoxic stress.

2. Materials and Methods

2.1 Mitochondrial extraction

Mitochondria were extracted from tissues of 10-13 weeks old female C57 BL/6OlaHsd mice using differential centrifugation and purification by sucrose gradient. The mice were sacrificed by cervical dislocation, the tissues extracted, rinsed and finely minced in ice-cold homogenization buffer (225 mM Mannitol, 75 mM Sucrose, 20 mM Tris pH 7,4, 10 mM EDTA, 1 mg/ml BSA, 1 mM DTT). For brain samples, the whole brain of the mice was used. As skeletal muscle, the diaphragm was chosen due to its consistent composition of red muscle fibers. Brown fat was isolated from the back of the mice avoiding any visible white fat contamination. Kidney and heart were used as whole organs, for liver only the biggest lobe.

The tissue suspensions were homogenized using a Dounce homogenizer and cell debris pelleted by centrifugation (2x 5 min 1000g, 4°C). A crude mitochondria preparation was pelleted from the supernatant (10 min 15.000g, 4°C), overlayed over a two-step sucrose gradient (1,5 M and 1 M sucrose in 10 mM HEPES pH 7,4, 10 mM EDTA, for brain mitochondria 0,8 M sucrose instead of 1 M) and subjected to ultracentrifugation (1h 50.000g, 4°C). The purified mitochondrial layer was recovered from the interphase of the two sucrose layers and used for extraction of mitochondrial proteins and nucleic acids.

2.2 Quantitative Western Blot Analysis for mtDNA Maintenance Protein Levels

Mitochondrial proteins were extracted from sucrose-purified mitochondria as described (Wanrooij et al, 2007) using TotEx buffer (20 mM HEPES pH 7,9, 400 mM NaCl, 20% glycerol, 1% IGEPAC, 1mM $MgCl_2$, 0,5 mM EDTA, 0,1 mM EGTA, 10 mM β-Glycerophosphate, 10 mM NaF, 9 mM DTT and 1x cOmplete EDTA-free protease inhibitor cocktail (Roche)) and protein concentration was determined by Bradford assay.

For Western blot analysis 75-150 µg of protein were separated on 8, 12 or 15% SDS-PAGE gels and transferred to nitrocellulose membranes (ProTran, Life Technologies). The membranes were blocked with 3% skim milk in low-salt TBST (50 mM TRIS pH 7,4, 150 mM NaCl, 0,1% Tween-20) for 1 h at room temperature. Primary antibodies were diluted in 3 % BSA in TBST buffer and incubated overnight at +4°C; secondary antibodies were prepared in TBST and incubated 1 hour at room temperature. Proteins were visualized by chemiluminescence detection (Mruk & Cheng, 2011), quantified and normalized to HSP60 content with Quantity One 4.6.2 software. To verify that equal protein amounts were analyzed one gel was cut into pieces before blotting. The gel part containing proteins between 80 and 120 kDa was stained with Coomassie (InstantBlue, Expedeon), scanned and the intensity of each lane was quantified with Quantity One 4.6.2 software. The lower part of the gel was blotted, cut into appropriate strips and probed with antibodies against VDAC, ATAD3, TOMM20, and SDHA. After chemiluminescent exposure the blots were extensively washed to remove the signal of the anti-rabbit secondary antibody and reprobed with mouse monoclonal antibodies against HSP60 and COXI.

Table 1: antibodies used for Western blots

rabbit-anti-mtSSB	1:1000	Sigma, HPA002866
rabbit-anti-ATAD3	1:25000	kind gift of Dr. Cooper
rabbit-anti-TFAM	1:1000	Abcam
rabbit-anti-TFB2M	1:1500	Abcam, ab66014
rabbit-anti-PolG1	1:500	Abcam, ab128899
rabbit-anti-PolRmt	1:500	Abcam, ab32988
mouse-anti-VDAC1	1:2000	Sigma, SAB5201374
rabbit-anti-TWNK(PEO1)	1:2000	antibodies online, ABIN2405996
rabbit-anti-Tomm20	1:5000	Sigma, HPA11562
mouse-anti-HSP60	1:20000	antibodies-online, ABIN361784
rabbit-anti-COXI	1:2000	Abcam ab14705
goat-anti-mouse IgG HRP	1:10.000	antibodies-online, ABIN101744
goat-anti-rabbit-IgG HRP	1:15.000	Life Technologies, A16104

2.3 Determination of mitochondrial copy number by quantitative PCR

Total DNA was extracted from tissues as described (Goffart et al., 2009). Relative levels of mtDNA copy number were determined in triplicates by TaqMan-based duplex real-time PCR using 100 ng DNA template, 300 nM nuclear NDUFV1 primers, 100 nM 16S primers and 125 nM of both probes in a final volume of 20 µl AccuTaq readymix (VWR). The reactions were denatured at 95°C for 3 min followed by 40 cycles of denaturation (95˚C for 20s), hybridization (52˚C for 20s) and elongation (72˚C for 20s) on an AriaMx realtime PCR system (Agilent Technologies).

NDUFV1forward 5´- CTT CCC CAC TGG CCT AA -3´

NDUFV1 reverse 5´- CCA AAA CCC AGT GAT CCA GC -3´

NDUFV1 probe 5´- VIC-GAG CCT TAG GGA AGA AGA GGC AG-MGBNFQ-3´

16S rRNA forward, 5´- TGC CTG CCC AGT GAC TAA AG -3´

16S rRNA reverse, 5´- GAC CCT CGT TTA GCC GTT CA-3´

16S rRNAprobe 5´-FAM-TGA CCG TGC AAA GGT AGC AT-MGBNFQ-3´

2.4 Determination of mitochondrial copy number per tissue protein mass

Tissue pieces of ca. 500 mg were homogenized by ultra-thurrax in homogenization buffer. 20 % of the homogenate was used to extract total protein with TOTEX buffer, the remaining 80 % were used to isolate DNA as described above. Total DNA and protein content of the samples were quantified and the relative mitochondrial copy number per protein calculated using mtDNA copy number per nuclear DNA and total DNA content per protein.

2.5 Determination of mitochondrial DNA topology and replication patterns

The conformation and replication intermediates of mtDNA were analyzed by one- and two-dimensional agarose gel electrophoresis and Southern blotting as described (Goffart et al., 2009). 1,5 µg mtDNA was used for topology gels and the blots were probed with a ^{32}P-labelled probe for *Nd2* (nts 3,774-4,571 of mouse mtDNA). For 2D-gels 5 µg of mtDNA were digested with *Cla*I and the blots were probed with a cytochrome C probe (nts 14783-15333). The radioactive signal was quantified using phosphorimager (BAS-IP MS screens, GE Healthcare, and Molecular Imager FX, BioRad) and X-ray film (Carestream Kodak MS).

2. 6 Northern blot analysis for determination of mitochondrial genes expression

Total RNA from tissues was extracted using TRI reagent (Sigma) following the manufacturer's recommendations. 4 µg of total RNA were separated over a 1.2% agarose MOPS/Formaldehyde gel and blotted using standard procedures. Mitochondrial RNA levels were quantified using *Nd1* (nts3,774-4,373), *Cytb* (nts 14783-15333), *Atp6* (nts 8165-8494) and *Nd5* (13,288-13,840) probes and normalized using a *28S* rRNA probe (nts 4,165-4,703 of *28S* rRNA) as a loading control.

2.7 Detection of mtDNA damage

Relative levels of polymerase-inhibiting DNA damage were determined in triplicates by a TaqMan-based long-range real-time PCR spanning the range from *16S* to *Atp6* of mouse mtDNA. The primers used for the longer PCR were mtDNA1978F (5´- TCC GAG CAT CTT ATC CAC GC -3´) and mtDNA8496R (5´- ACC ATT TCT AGG ACA ATG GGC A -3´). The PCR was performed in 20 µl reactions containing 100 ng DNA template, 500 nM mtDNA primers, 125 nM *16S* probe and 1xAccuTaq Readymix (VWR). The reactions were denatured at 94°C for 5 min followed by 40 cycles of denaturation (94°C for 20 s), hybridization (64°C for 20 s) and elongation (72°C for 7 min) on an AriaMx realtime PCR system (Agilent Technologies). The template amount was quantified using the above described quantitative PCR for 16S and the relative damage in different samples was calculated as described in (Lehle et al., 2014), using the average of three liver samples as reference.

3. Results and Discussion

3.1 Mitochondrial DNA copy number and organization

While the mitochondrial mass, metabolism and respiratory capacity of different mammalian tissues is expected to vary a lot, the true extent and nature of these differences is not clear as the normalization of data from different tissues is extremely challenging (Fernandez-Vizarra et al., 2011). Different tissues and cell types have completely different gene expression profiles, including the so-called housekeeping genes generally used to normalize the results when expression profiles of genes of interest are studied. In addition, alterations in total gene expression activity between cell types makes proportional comparisons difficult, as cells having identical mitochondrial mass and expression of mitochondrial genes might differ in their total gene or protein expression levels.

Although mitochondrial DNA levels are often used as a marker of mitochondrial mass or activity, its relevance to mitochondrial functions is unclear (Pohjoismaki, 2012; Pohjoismaki et al., 2013a). As with protein and gene expression levels, normalization of mitochondrial DNA copy number between different tissues samples is challenging. A standard procedure is to measure mtDNA per nuclear gene copy, however this does not take the cell size into account, that can vary considerably (Pohjoismaki et al., 2013a). For example the growth of cardiomyocytes during post-natal heart development is responsible for an increase in mtDNA:nDNA ratio, although the mtDNA copy number per tissue volume is kept constant (Pohjoismaki et al., 2013a) and the increase in mitochondrial OXPHOS complexes is actually caused by an increase in mtDNA gene expression (Pohjoismaki et al., 2012).

To overcome this quantification problem we aimed to compare the levels of mtDNA maintenance factors to an appropriate reference. Our initial approach was to normalize the expression levels of mitochondrial genes of interest against transcripts such as *Hprt* or *SDHA*, which have relatively stable expression levels across different rodent tissues (Svingen et al., 2015). However, also their expression varies depending on the physiological conditions and treatments in C57BL/6 mice (Gong et al., 2016) and was found unreliable for some tissues, such as brain and brown fat. More importantly, the measured transcript levels correlated poorly with the observed protein levels (Supplementary Fig. and Fig.3/4). Instead, we sought to reveal the qualitative differences on protein level by comparing mitochondrial protein extracts from the analyzed tissues in contrast to using total tissue lysates. Besides controlling the level of total mitochondrial protein, we decided to normalize the protein levels against mitochondrial chaperonin, HSP60. Our reasoning was that as HSP60 is required for the mitochondrial protein import, its levels should correspond to this requirement quantitatively, regardless of the type of the mitochondrial proteins. HSP60 is also required for the

mitochondrial protein quality control (Voos et al., 2016), potentially causing a bias for tissues with high protein turnover. However, in our hands, brain, heart, liver, muscle, kidney and brown fat from 10-13 weeks old mice showed remarkably similar basal levels of HSP60, when compared to the total mitochondrial protein (Fig 1), with only liver containing elevated levels of HSP60 compared to all other tissues. Also the mitochondrial AAA+-ATPase ATAD3 correlated very well with the overall mitochondrial protein mass, thus offering an alternative reference, while the expression of SDHA, TOMM20, VDAC or the mitochondrial encoded complex I-subunit COXI were showing variation between the tissues (Fig 1).

When comparing mtDNA levels in different adult mouse tissues we found brown fat to have the highest mtDNA copy number per cell (Fig. 2A), but no differences in mtDNA copy numbers between tissues when normalizing mtDNA levels per protein as an indicator of tissue mass (Fig. 2B). Mitochondrial DNA topology instead showed clear differences in the investigated tissues: mtDNA from brain and liver was mainly present in relaxed open-circle conformation, while heart, muscle, kidney and brown fat mtDNA had high levels of linear mtDNA molecules and dimers (Fig. 2C). In addition, 7S levels were rather comparable with only brown adipose tissue being slightly lower than the other cell types. (Fig. 2D).

Human mtDNA can exist as supercoiled or relaxed circle, as a linear molecule or as a circular dimer (Kolesar et al., 2013). Additionally two or more circular molecules might be interlinked as catenanes. All these topological forms of mtDNA are also found in mouse tissues (Fig. 2C), but interestingly the differences in the relative quantities are less extreme than found in humans (Pohjoismaki et al., 2009). In mouse heart, muscle, kidney and brown fat mtDNA have very comparable ratios of the different topology forms, whereas liver and brain have mainly simple circular monomers. Brain mtDNA additionally possesses

heterogeneous complex forms (hmw3), which migrate poorly during electrophoresis and seem to lack a faster migrating catenane form (hmw1), present in most tissues. For the assignment of the different topological forms, please see Pohjoismäki *et al.* (Pohjoismaki et al., 2009) and Kolesar *et al.* (Kolesar et al., 2013).

3.2 Tissue-specific features of mtDNA replication and recombination

As pointed out earlier, mammalian mitochondria have two types of mtDNA replication intermediates. The strand-asynchronous replication (RITOLS) intermediates are the predominant type in cultured cells (Pohjoismaki and Goffart, 2011) and represents the best-studied mechanism that can also be modeled *in vitro* (Korhonen et al., 2004). In this type of replication, the heavy strand (named after its nucleotide content) is replicated first, resulting in the displacement of the light strand template. This displaced strand is initially covered with RNA and replicated with a delay (Reyes et al., 2013; Yasukawa et al., 2006). In two-dimensional agarose gel analysis these RNA:DNA hybrid molecules have distinctive migration characteristics compared to double-strand DNA replication intermediates (Pohjoismaki et al., 2010). Replication initiating at the origin of heavy strand replication (O_H) will result in growing replication bubble that converts to y- or y-like forked forms when the replication reaches the end of the restriction fragment. RNA:DNA hybrid containing replication bubbles will form a characteristic blunted bubble arc due to slight degradation (Pohjoismaki et al., 2010) (Fig. 3A), whereas dsDNA replication bubbles, originating from strand-coupled replication, migrate as sharper arc (Wanrooij et al., 2007) (Fig. 3B). MtDNA molecules undergoing cross-over events migrate on a line named x-arc, but it is currently unclear whether these recombination events in mouse cells are part of replication as described for human heart (Pohjoismaki et al., 2009) or rather a sign of mtDNA repair (Fig. 3B, dashed line).

In mouse, we could identify three different tissue specific patterns of mtDNA replication. Kidney and liver mtDNA have high levels of classical strand-asynchronous replication intermediates characterized by a blunt, shorter bubble arc (Fig. 3D), whereas heart and brain show the defined, long bubble arc and the absence of slow moving y-arcs typical for COSCOFA replication (Fig. 3E). Brain also contains extremely high levels of x-shaped recombination intermediates forming an x-spike, while these are visible, but less prominent in heart.

Skeletal muscle shows predominantly RITOLS intermediates, visible as blunt bubble arc and slow moving y-arc, but additionally possesses a clear x-spike indicating mtDNA recombination (Fig. 3F). MtDNA in brown adipose tissue seems to employ both RITOLS and COSCOFA replication, as both blunt and sharp bubble arc are detected. Also this tissue contains a high proportion of recombining mtDNA intermediates (Fig. 3F).

3.3 mtDNA damage

During post-natal development human heart acquires high levels of mtDNA recombination (Pohjoismaki et al., 2009), most likely as an adaptation against elevated oxidative stress in the metabolically active adult heart (Pohjoismaki et al., 2013a). As oxidative stress could also induce the mtDNA recombination we found in several mouse tissues, we measured the levels of mtDNA lesions in the different tissues (Fig. 3G). As the method is PCR-based, it detects any damage causing Taq-polymerase to stall, such as abasic sites, RNA incorporation, nucleotide dimers, but does not detect 8-oxoG, a marker that is frequently used to assess oxidative DNA damage but leads to mutations rather than arrest of the replication fork.

The lowest levels of mtDNA damage were found in liver and kidney cells, then highest in brain and adipose tissue (Fig 3G). This mtDNA damage correlated well with the presence of

recombination intermediates (Fig. 3D-F); corroborating with the idea that recombination might be an adaptation against intrinsic mtDNA damage (Pohjoismaki et al., 2009; Pohjoismaki et al., 2013b). Most mtDNA damage was present in brown fat cells, having a high mitochondrial content and an active mitochondrial energy metabolism (Johnson et al., 2007a; Johnson et al., 2007b). In addition, brain tissue showed relatively many mtDNA lesions, but as brain consists of various cell types with different mitochondrial metabolism the interpretation is more difficult. The predominant cells in neural tissue are astrocytes and neurons. While the former depend mainly on glycolysis, they also produce higher levels of ROS than neurons (Lopez-Fabuel et al., 2016), which depend strictly on oxidative phosphorylation but have low levels of antioxidants (Herrero-Mendez et al., 2009). Our results suggest that both of these cell types have a high incidence of mtDNA lesions, and likely the same cells employ mtDNA recombination to maintain the integrity of their mtDNA pool. The maintenance of mtDNA in neurons is likely to be more critical as they are post-mitotic and cannot be replaced, whereas astrocytes can proliferate. Fittingly, the accumulation of mtDNA deletions specifically in neurons is connected to neurodegenerative diseases (Neuhaus et al., 2014; Neuhaus et al., 2017; Stefanatos and Sanz, 2017). The lowest rate of mtDNA lesions was detected in liver and kidney, both tissues that are able to regenerate *via* cellular proliferation (Han et al., 2015; Rinkevich et al., 2014). The same tissues did not show any sign of mtDNA recombination, suggesting that this process might be employed mainly by post-mitotic cells as an adaptation to increased levels of mtDNA damage.

3.4 Mitochondrial replisome components

To elucidate the reasons behind the striking differences in mtDNA replication mechanisms in the investigated tissues we aimed to quantify the expression of known mitochondrial

replisome components. Of the main components, replicative helicase TWNK was equally expressed in heart, skeletal muscle, liver, kidney and brown fat, although differences in the presence of two isoforms were detected (Fig. 3H). In brain, no signal was detected at the height of the monomeric TWNK protein, although two different antibodies detected an abundant higher molecular weight protein (ca. 120 kDa) that might be an unknown isoform or a non-denatured multimer of TWNK (Spelbrink et al., 2001). Mitochondrial SSB levels in contrast were highest in liver and kidney, although the protein could be detected at low levels also in all other tissues (Fig 3H). Also the levels of the catalytic subunit of mitochondrial polymerase Polγ were surprisingly variable (Fig 3H). Most POLG1 was found in heart and liver. A low amount of POLG was also present in kidney mitochondria, while brain, muscle and brown fat had proteins levels below the detection limit. As the gene is clearly expressed in all studied tissues (suppl. Fig.) the large differences in protein level might be due to translational or protein stability differences.

The fact that mtSSB is most abundant in tissues that employ the asynchronous replication mode is interesting, as there is an ongoing debate whether during the asynchronous replication of mtDNA the lagging strand is covered by mtSSB (Miralles Fuste et al., 2014) or RNA (Pohjoismaki et al., 2010; Reyes et al., 2013). While the 2D pattern clearly indicates the presence of RNA-containing intermediates (see Reyes *et al.* 2013 for detailed explanations) our data still suggests an important role of mtSSB for RITOLS replication. Although the mechanism has not yet been elucidated, the RNA:DNA hybridization at the mitochondrial replication fork has to be an active process, mediated by an enzyme. mtSSB might be required for stabilization displaced strand to allow the annealing of the preformed RNA. Interestingly, the knockdown of mtSSB has only minor effects on mtDNA copy number, suggesting that its role for the stabilization of the displaced strand is at least partially redundant (Ruhanen et al., 2010).

3.4 Mitochondrial gene expression

Previous work (Reyes et al., 2013) has shown that RNA:DNA hybrid replication intermediates are generated by recruitment of preformed processed mitochondrial transcripts, thus suggesting that mitochondrial replication and transcription might be linked indirectly. To assess whether replication mode is regulated by the amount of available RNA molecules we quantified the steady-state levels of several mitochondrial transcripts. Our results confirmed the existing knowledge that there is a large variation in mitochondrial gene expression between different cell types. Of the studied tissues heart and brown fat contained the highest levels of mitochondrial transcripts compared to *28S* ribosomal RNA (Fig 4A), while the other tissues possess significantly lower mitochondrial expression. As heart tissue, possessing the highest mitochondrial transcript levels, is exclusively employing strand-coupled replication (Fig. 4A and 3B), it can be concluded that the abundance of mitochondrial transcripts does not correlate with the strand-asynchronous replication in the investigated tissues.

The mitochondrial RNA polymerase POLRMT is not only synthetizing mitochondrial transcripts, but also acts as primase during replication (Wanrooij et al., 2008) and thus should be especially required during strand-coupled replication that involves frequent priming of Okazaki fragments on the lagging strand. We thus compared the amounts of POLRMT as well as the mitochondrial transcription factors TFAM and TFB2M in the different tissues (Fig. 4B), but the detected protein levels did correlate neither with the observed replication mode (Fig. 3D-F) nor with the steady-state levels of transcripts (Fig. 4A), suggesting that the abundance of the transcription machinery does not regulate mtDNA maintenance.

4. Concluding Remarks

In the presented study, we sought to elucidate the tissue-specific differences in mammalian mitochondrial maintenance, hoping to provide better background for the understanding of the tissue specificity of many mitochondrial diseases. We found that there are substantial differences in mtDNA replication mechanisms between tissues. While these differences are not correlated with mtDNA copy number, topology or gene expression, we found tissues with higher loads of mtDNA damage to rely on strand-coupled replication and use mtDNA recombination, while tissues with potentially low oxidative environment tend to replicate their mtDNA via a strand-asynchronous mechanism. Thus, the strand-coupled mechanism of mitochondrial DNA replication is likely to represent an adaptation to the presence of oxidative stress, as previously suggested (Torregrosa-Munumer et al., 2015). As mtDNA maintenance disorders most commonly affect tissues like muscle and brain, showing higher levels of DNA damage and replicate *via* the strand-coupled mechanism, it is possible that part of the disease phenotype is caused by the failure to maintain genome integrity in a highly oxidative environment. It remains a challenge for the future to discover the regulators that govern the switch between the two different replication modes.

5. Acknowledgements

The polyclonal antibody against ATAD3 was a kind gift from Dr. Helen Cooper, Åbo Akademi, Turku, Finland. We thank the Laboratory animal facility of the University of Eastern Finland for their flexible support.

6. Author Contributions

EH, NJK, AH and SG performed the experiments, EH, JLP and SG wrote the manuscript, SG designed the study.

7. Conflicts of interest

The authors do not declare any conflicts of interests.

8. Funding sources

EH, NK, AH and SG were supported by the Academy of Finland (grants No. 292822 and 265314), AH also by the Finnish Cultural Foundation, North Carelia Regional fund (grant No.55172179). JLP received funding by the Jane and Aatos Erkko foundation. The funding sources did not participate in the research or publication process.

9. References

Alston, C.L., Rocha, M.C., Lax, N.Z., Turnbull, D.M., Taylor, R.W., 2017. The genetics and pathology of mitochondrial disease. The Journal of pathology 241, 236-250.

Ciesielski, G.L., Oliveira, M.T., Kaguni, L.S., 2016. Animal Mitochondrial DNA Replication. The Enzymes 39, 255-292.

Crews, S., Ojala, D., Posakony, J., Nishiguchi, J., Attardi, G., 1979. Nucleotide sequence of a region of human mitochondrial DNA containing the precisely identified origin of replication. Nature 277, 192-198.

Ekstrand, M.I., Falkenberg, M., Rantanen, A., Park, C.B., Gaspari, M., Hultenby, K., Rustin, P., Gustafsson, C.M., Larsson, N.G., 2004. Mitochondrial transcription factor A regulates mtDNA copy number in mammals. Human molecular genetics 13, 935-944.

Falkenberg, M., Larsson, N.G., Gustafsson, C.M., 2007. DNA replication and transcription in mammalian mitochondria. Annual review of biochemistry 76, 679-699.

Fernandez-Vizarra, E., Enriquez, J.A., Perez-Martos, A., Montoya, J., Fernandez-Silva, P., 2011. Tissue-specific differences in mitochondrial activity and biogenesis. Mitochondrion 11, 207-213.

Fish, J., Raule, N., Attardi, G., 2004. Discovery of a major D-loop replication origin reveals two modes of human mtDNA synthesis. Science 306, 2098-2101.

Fukuoh, A., Ohgaki, K., Hatae, H., Kuraoka, I., Aoki, Y., Uchiumi, T., Jacobs, H.T., Kang, D., 2009. DNA conformation-dependent activities of human mitochondrial RNA polymerase. Genes to cells : devoted to molecular & cellular mechanisms 14, 1029-1042.

Fuste, J.M., Wanrooij, S., Jemt, E., Granycome, C.E., Cluett, T.J., Shi, Y., Atanassova, N., Holt, I.J., Gustafsson, C.M., Falkenberg, M., 2010. Mitochondrial RNA polymerase is needed for activation of the origin of light-strand DNA replication. Molecular cell 37, 67-78.

Goffart, S., Cooper, H.M., Tyynismaa, H., Wanrooij, S., Suomalainen, A., Spelbrink, J.N., 2009. Twinkle mutations associated with autosomal dominant progressive external ophthalmoplegia lead to impaired helicase function and in vivo mtDNA replication stalling. Human molecular genetics 18, 328-340.

Gong, H., Sun, L., Chen, B., Han, Y., Pang, J., Wu, W., Qi, R., Zhang, T.M., 2016. Evaluation of candidate reference genes for RT-qPCR studies in three metabolism related tissues of mice after caloric restriction. Scientific reports 6, 38513.

Han, L.H., Dong, L.Y., Yu, H., Sun, G.Y., Wu, Y., Gao, J., Thasler, W., An, W., 2015. Deceleration of liver regeneration by knockdown of augmenter of liver regeneration gene is associated with impairment of mitochondrial DNA synthesis in mice. American journal of physiology. Gastrointestinal and liver physiology 309, G112-122.

Herrero-Mendez, A., Almeida, A., Fernandez, E., Maestre, C., Moncada, S., Bolanos, J.P., 2009. The bioenergetic and antioxidant status of neurons is controlled by continuous degradation of a key glycolytic enzyme by APC/C-Cdh1. Nature cell biology 11, 747-752.

Jayashankar, V., Mueller, I.A., Rafelski, S.M., 2016. Shaping the multi-scale architecture of mitochondria. Current opinion in cell biology 38, 45-51.

Johnson, D.T., Harris, R.A., Blair, P.V., Balaban, R.S., 2007a. Functional consequences of mitochondrial proteome heterogeneity. American journal of physiology. Cell physiology 292, C698-707.

Johnson, D.T., Harris, R.A., French, S., Blair, P.V., You, J., Bemis, K.G., Wang, M., Balaban, R.S., 2007b. Tissue heterogeneity of the mammalian mitochondrial proteome. American journal of physiology. Cell physiology 292, C689-697.

Kanki, T., Ohgaki, K., Gaspari, M., Gustafsson, C.M., Fukuoh, A., Sasaki, N., Hamasaki, N., Kang, D., 2004. Architectural role of mitochondrial transcription factor A in maintenance of human mitochondrial DNA. Molecular and cellular biology 24, 9823-9834.

Kolesar, J.E., Wang, C.Y., Taguchi, Y.V., Chou, S.H., Kaufman, B.A., 2013. Two-dimensional intact mitochondrial DNA agarose electrophoresis reveals the structural complexity of the mammalian mitochondrial genome. Nucleic acids research 41, e58.

Korhonen, J.A., Pham, X.H., Pellegrini, M., Falkenberg, M., 2004. Reconstitution of a minimal mtDNA replisome in vitro. The EMBO journal 23, 2423-2429.

Kukat, C., Davies, K.M., Wurm, C.A., Spahr, H., Bonekamp, N.A., Kuhl, I., Joos, F., Polosa, P.L., Park, C.B., Posse, V., Falkenberg, M., Jakobs, S., Kuhlbrandt, W., Larsson, N.G., 2015. Cross-strand binding of TFAM to a single mtDNA molecule forms the mitochondrial nucleoid. Proceedings of the National Academy of Sciences of the United States of America 112, 11288-11293.

Kunz, W.S., 2003. Different metabolic properties of mitochondrial oxidative phosphorylation in different cell types--important implications for mitochondrial cytopathies. Experimental physiology 88, 149-154.

Lehle, S., Hildebrand, D.G., Merz, B., Malak, P.N., Becker, M.S., Schmezer, P., Essmann, F., Schulze-Osthoff, K., Rothfuss, O., 2014. LORD-Q: a long-run real-time PCR-based DNA-damage quantification method for nuclear and mitochondrial genome analysis. Nucleic acids research 42, e41.

Lopez-Fabuel, I., Le Douce, J., Logan, A., James, A.M., Bonvento, G., Murphy, M.P., Almeida, A., Bolanos, J.P., 2016. Complex I assembly into supercomplexes determines differential mitochondrial ROS production in neurons and astrocytes. Proceedings of the National Academy of Sciences of the United States of America 113, 13063-13068.

Matsushima, Y., Goto, Y., Kaguni, L.S., 2010. Mitochondrial Lon protease regulates mitochondrial DNA copy number and transcription by selective degradation of mitochondrial transcription factor A (TFAM). Proceedings of the National Academy of Sciences of the United States of America 107, 18410-18415.

Miralles Fuste, J., Shi, Y., Wanrooij, S., Zhu, X., Jemt, E., Persson, O., Sabouri, N., Gustafsson, C.M., Falkenberg, M., 2014. In vivo occupancy of mitochondrial single-stranded DNA binding protein supports the strand displacement mode of DNA replication. PLoS genetics 10, e1004832.

Neuhaus, J.F., Baris, O.R., Hess, S., Moser, N., Schroder, H., Chinta, S.J., Andersen, J.K., Kloppenburg, P., Wiesner, R.J., 2014. Catecholamine metabolism drives generation of mitochondrial DNA deletions in dopaminergic neurons. Brain : a journal of neurology 137, 354-365.

Neuhaus, J.F., Baris, O.R., Kittelmann, A., Becker, K., Rothschild, M.A., Wiesner, R.J., 2017. Catecholamine Metabolism Induces Mitochondrial DNA Deletions and Leads to Severe Adrenal Degeneration during Aging. Neuroendocrinology 104, 72-84.

Pham, X.H., Farge, G., Shi, Y., Gaspari, M., Gustafsson, C.M., Falkenberg, M., 2006. Conserved sequence box II directs transcription termination and primer formation in mitochondria. The Journal of biological chemistry 281, 24647-24652.

Pohjoismaki, J.L., 2012. Letter by Pohjoismaki regarding article, "Impaired mitochondrial biogenesis precedes heart failure in right ventricular hypertrophy in congenital heart disease". Circulation. Heart failure 5, e15; author reply e16.

Pohjoismaki, J.L., Boettger, T., Liu, Z., Goffart, S., Szibor, M., Braun, T., 2012. Oxidative stress during mitochondrial biogenesis compromises mtDNA integrity in growing hearts and induces a global DNA repair response. Nucleic acids research 40, 6595-6607.

Pohjoismaki, J.L., Goffart, S., 2011. Of circles, forks and humanity: Topological organisation and replication of mammalian mitochondrial DNA. BioEssays : news and reviews in molecular, cellular and developmental biology 33, 290-299.

Pohjoismaki, J.L., Goffart, S., 2017. The role of mitochondria in cardiac development and protection. Free radical biology & medicine.

Pohjoismaki, J.L., Goffart, S., Tyynismaa, H., Willcox, S., Ide, T., Kang, D., Suomalainen, A., Karhunen, P.J., Griffith, J.D., Holt, I.J., Jacobs, H.T., 2009. Human heart mitochondrial DNA is organized in

complex catenated networks containing abundant four-way junctions and replication forks. The Journal of biological chemistry 284, 21446-21457.
Pohjoismaki, J.L., Holmes, J.B., Wood, S.R., Yang, M.Y., Yasukawa, T., Reyes, A., Bailey, L.J., Cluett, T.J., Goffart, S., Willcox, S., Rigby, R.E., Jackson, A.P., Spelbrink, J.N., Griffith, J.D., Crouch, R.J., Jacobs, H.T., Holt, I.J., 2010. Mammalian mitochondrial DNA replication intermediates are essentially duplex but contain extensive tracts of RNA/DNA hybrid. J Mol Biol 397, 1144-1155.
Pohjoismaki, J.L., Kruger, M., Al-Furoukh, N., Lagerstedt, A., Karhunen, P.J., Braun, T., 2013a. Postnatal cardiomyocyte growth and mitochondrial reorganization cause multiple changes in the proteome of human cardiomyocytes. Mol Biosyst 9, 1210-1219.
Pohjoismaki, J.L., Wanrooij, S., Hyvarinen, A.K., Goffart, S., Holt, I.J., Spelbrink, J.N., Jacobs, H.T., 2006. Alterations to the expression level of mitochondrial transcription factor A, TFAM, modify the mode of mitochondrial DNA replication in cultured human cells. Nucleic acids research 34, 5815-5828.
Pohjoismaki, J.L., Williams, S.L., Boettger, T., Goffart, S., Kim, J., Suomalainen, A., Moraes, C.T., Braun, T., 2013b. Overexpression of Twinkle-helicase protects cardiomyocytes from genotoxic stress caused by reactive oxygen species. Proceedings of the National Academy of Sciences of the Unite d States of America 110, 19408-19413.
Reyes, A., Kazak, L., Wood, S.R., Yasukawa, T., Jacobs, H.T., Holt, I.J., 2013. Mitochondrial DNA replication proceeds via a 'bootlace' mechanism involving the incorporation of processed transcripts. Nucleic acids research 41, 5837-5850.
Rinkevich, Y., Montoro, D.T., Contreras-Trujillo, H., Harari-Steinberg, O., Newman, A.M., Tsai, J.M., Lim, X., Van-Amerongen, R., Bowman, A., Januszyk, M., Pleniceanu, O., Nusse, R., Longaker, M.T., Weissman, I.L., Dekel, B., 2014. In vivo clonal analysis reveals lineage-restricted progenitor characteristics in mammalian kidney development, maintenance, and regeneration. Cell reports 7, 1270-1283.
Rubio-Cosials, A., Sidow, J.F., Jimenez-Menendez, N., Fernandez-Millan, P., Montoya, J., Jacobs, H.T., Coll, M., Bernado, P., Sola, M., 2011. Human mitochondrial transcription factor A induces a U-turn structure in the light strand promoter. Nature structural & molecular biology 18, 1281-1289.
Ruhanen, H., Borrie, S., Szabadkai, G., Tyynismaa, H., Jones, A.W., Kang, D., Taanman, J.W., Yasukawa, T., 2010. Mitochondrial single-stranded DNA binding protein is required for maintenance of mitochondrial DNA and 7S DNA but is not required for mitochondrial nucleoid organisation. Biochimica et biophysica acta 1803, 931-939.
Scarpulla, R.C., 2008. Nuclear control of respiratory chain expression by nuclear respiratory factors and PGC-1-related coactivator. Annals of the New York Academy of Sciences 1147, 321-334.
Schrepfer, E., Scorrano, L., 2016. Mitofusins, from Mitochondria to Metabolism. Molecular cell 61, 683-694.
Sen, D., Nandakumar, D., Tang, G.Q., Patel, S.S., 2012. Human mitochondrial DNA helicase TWINKLE is both an unwinding and annealing helicase. The Journal of biological chemistry 287, 14545-14556.
Sen, D., Patel, G., Patel, S.S., 2016. Homologous DNA strand exchange activity of the human mitochondrial DNA helicase TWINKLE. Nucleic acids research 44, 4200-4210.
Shi, Y., Dierckx, A., Wanrooij, P.H., Wanrooij, S., Larsson, N.G., Wilhelmsson, L.M., Falkenberg, M., Gustafsson, C.M., 2012. Mammalian transcription factor A is a core component of the mitochondrial transcription machinery. Proceedings of the National Academy of Sciences of the United States of America 109, 16510-16515.
Spelbrink, J.N., Li, F.Y., Tiranti, V., Nikali, K., Yuan, Q.P., Tariq, M., Wanrooij, S., Garrido, N., Comi, G., Morandi, L., Santoro, L., Toscano, A., Fabrizi, G.M., Somer, H., Croxen, R., Beeson, D., Poulton, J., Suomalainen, A., Jacobs, H.T., Zeviani, M., Larsson, C., 2001. Human mitochondrial DNA deletions associated with mutations in the gene encoding Twinkle, a phage T7 gene 4-like protein localized in mitochondria. Nat Genet 28, 223-231.
Stefanatos, R., Sanz, A., 2017. The role of mitochondrial ROS in the aging brain. FEBS letters.

Svingen, T., Letting, H., Hadrup, N., Hass, U., Vinggaard, A.M., 2015. Selection of reference genes for quantitative RT-PCR (RT-qPCR) analysis of rat tissues under physiological and toxicological conditions. PeerJ 3, e855.

Torregrosa-Munumer, R., Forslund, J.M.E., Goffart, S., Pfeiffer, A., Stojkovic, G., Carvalho, G., Al-Furoukh, N., Blanco, L., Wanrooij, S., Pohjoismaki, J.L.O., 2017. PrimPol is required for replication reinitiation after mtDNA damage. Proceedings of the National Academy of Sciences of the United States of America 114, 11398-11403.

Torregrosa-Munumer, R., Goffart, S., Haikonen, J.A., Pohjoismaki, J.L., 2015. Low doses of ultraviolet radiation and oxidative damage induce dramatic accumulation of mitochondrial DNA replication intermediates, fork regression, and replication initiation shift. Mol Biol Cell 26, 4197-4208.

Tyynismaa, H., Sembongi, H., Bokori-Brown, M., Granycome, C., Ashley, N., Poulton, J., Jalanko, A., Spelbrink, J.N., Holt, I.J., Suomalainen, A., 2004. Twinkle helicase is essential for mtDNA maintenance and regulates mtDNA copy number. Human molecular genetics 13, 3219-3227.

Wanrooij, S., Fuste, J.M., Farge, G., Shi, Y., Gustafsson, C.M., Falkenberg, M., 2008. Human mitochondrial RNA polymerase primes lagging-strand DNA synthesis in vitro. Proceedings of the National Academy of Sciences of the United States of America 105, 11122-11127.

Wanrooij, S., Goffart, S., Pohjoismaki, J.L., Yasukawa, T., Spelbrink, J.N., 2007. Expression of catalytic mutants of the mtDNA helicase Twinkle and polymerase POLG causes distinct replication stalling phenotypes. Nucleic acids research 35, 3238-3251.

Voos, W., Jaworek, W., Wilkening, A., Bruderek, M., 2016. Protein quality control at the mitochondrion. Essays in biochemistry 60, 213-225.

Yasukawa, T., Reyes, A., Cluett, T.J., Yang, M.Y., Bowmaker, M., Jacobs, H.T., Holt, I.J., 2006. Replication of vertebrate mitochondrial DNA entails transient ribonucleotide incorporation throughout the lagging strand. The EMBO journal 25, 5358-5371.

Figure legends

Fig. 1. Normalization of mitochondrial protein mass. (A) Western blot analysis of mitochondrial proteins suitable as loading reference for total mitochondrial protein content. The high molecular weight part of an SDS PAGE gel loaded with mitochondrial protein extracts from six different tissues was stained with Coomassie Brilliant blue to assess protein loading, while the lower part was Western blotted and probed with various antibodies detecting abundant mitochondrial proteins. (B) Quantification of the Western blots in (A) using the intensity of Coomassie staining for normalization. Western blot quantification of HSP60, SDHA and ATAD3 show a good correlation with total mitochondrial protein mass determined by Coomassie staining and are thus suitable as loading controls proteins, while the levels of TOMM20, COXI and VDAC in mitochondria of different cell types are variable. B = brain tissue, H = Heart, M = skeletal muscle, L = liver, K = kidney, BAT = brown fat tissue.

Fig. 2. Mitochondrial DNA levels in different tissues of adult mice. (A) Relative mtDNA copy number per nucleus normalized to liver tissue. Brown fat cells have significantly higher mtDNA content compared to liver and kidney (n=4, ANOVA with post-hoc Bonferroni inference). (B) Relative mtDNA copy number per total protein content. No significant difference between the investigated tissues was found (ANOVA). (C) mtDNA topology from the same tissues. The different topological forms can be identified as follows: Three different high molecular weight forms (hmw1–3), representing catenanes, dimers and recombining molecules; open circular monomers (oc), linear mtDNA (16.3 kb in mouse) and supercoiled monomers (sc). (D) 7S DNA levels from the same tissues, normalized against mtDNA copy

number. The only significant differences were found between skeletal muscle vs. BAT (ANOVA/Bonferroni, $p<0,01$) and kidney vs BAT ($p<0,05$).

Fig. 3. Mitochondrial DNA replication, recombination and mtDNA damage in different mouse tissues. (A-B) 2D-AGE patterns formed by the different replication modes. 2D-AGE separates DNA molecules according to their size (first dimension) and shape (second dimension). The majority of DNA consists of linear non-replicating molecules migrating as the fastest species in both dimensions (1n), while non-linear replication intermediates form various arcs depending on their structure. (A) Strand asynchronous mode replication initiates at O_H and initially only the leading strand is replicated, while the lagging strand is covered with RNA. This results in growing bubble structures that are sensitive to degradation and form a club-headed, partially single-stranded (pssb) bubble arc. When the replication exits the fragment, replication bubbles are converted into y-shaped structures that migrate on the descending y-arc (Y). As the fork of the y-shaped molecules is arresting at O_H, Y will not reach the linear arc. The incorporation of ribonucleotides occasionally blocks the restriction, leading to single-cut full-length mtDNA molecules migrating on the slow-moving y-arc (smY). (B) The strand-coupled replication mode produces fully double-stranded replication intermediates that are resistant to degradation (dsb). Thus, the formed bubble arc is a sharp line and extends longer. As this type of replication can initiate in a broad zone upstream of O_H also outside of the analyzed fragment, y-shaped molecules with shorter replicated arms are abundant, leading to a more visible ascending y-arc. Recombining mtDNA fragments containing a Holliday junction migrate in the first dimension according to their 2n size, forming a steep x-spike during the second dimension (dashed line). The formation of these x-fragments might not require replication at all and is not connected to the COSCOFA replication mode. (C) Details of the *Cla*I-digest used in panel D-F. (D) mtDNA in mouse

liver and kidney replicates *via* the strand-asynchronous replication mode characterized by a blunt bubble arc and slowly migrating smY. Partially degraded replication intermediates form a strong streak reaching from the 1n spot towards the tip of the y-arc. (E) Heart and brain tissue mtDNA employs strand-coupled replication as indicated by the defined, long bubble arc, the near absence of smY. A prominent x-spike is present in both tissues, indicating high levels of mtDNA recombination. (F) Skeletal muscle and brown fat mtDNA constitutes a mixture of strand-asynchronous (blunt bubble arc and smY) and strand-coupled (faint extended bubble arc, strong ascending y) replication intermediates together with intermediate levels of recombination (x-spike). (G) Quantification of PCR-inhibiting mtDNA damage by real-time long-range PCR using liver as reference. Brain and brown fat tissue show the highest load of mtDNA damage, while liver and kidney have the lowest (n=3, $p<0,05$ for brown fat compared to all other tissues but brain, liver vs. brain, ANOVA/Bonferroni). (H) Mitochondrial replisome components across different mouse tissues. Western blots of mitochondrial protein extracts from mouse brain (B), heart (H), skeletal muscle (M),liver (L), kidney (K) and brown adipose tissue (BAT), probed with Polγ1 (POLG1), TWNK and mtSSB antibodies with HSP60 as a loading control.

Fig. 4. Mitochondrial transcription in different tissues. (A) Steady-state transcript levels of *Nd1*, *Nd5*, *Atp6* and *Cytb* mRNAs quantified by Northern blot. Heart and brown adipose tissue possess significantly higher mitochondrial transcript levels compared to the other tissues. (n=3, ANOVA/Bonferroni; * $p<0,05$, ** $p<0,01$). (B) Western blot quantification of proteins involved in mitochondrial transcription. B = brain tissue, H = Heart, M = skeletal muscle, L = liver, K = kidney, BAT = brown fat tissue.

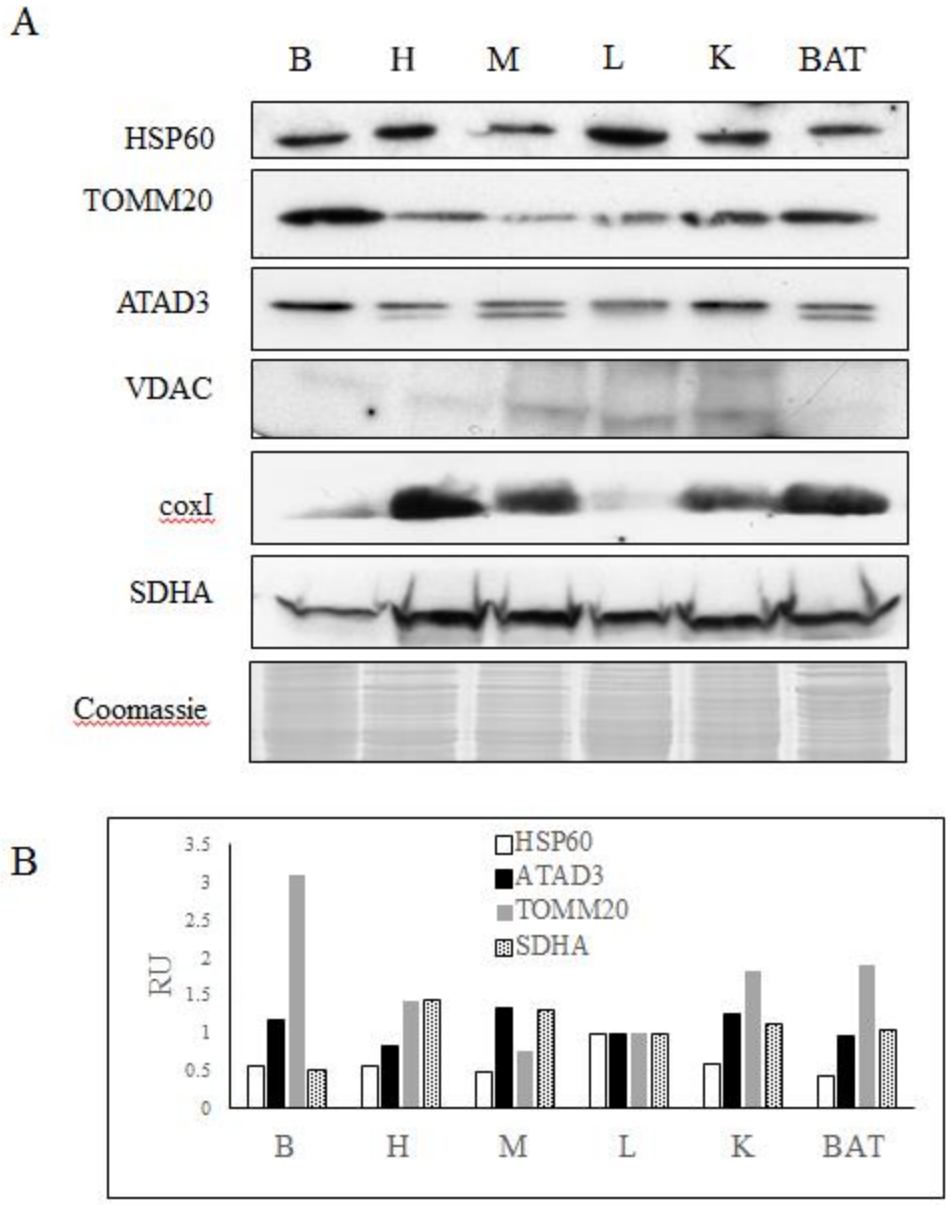

Figure 1

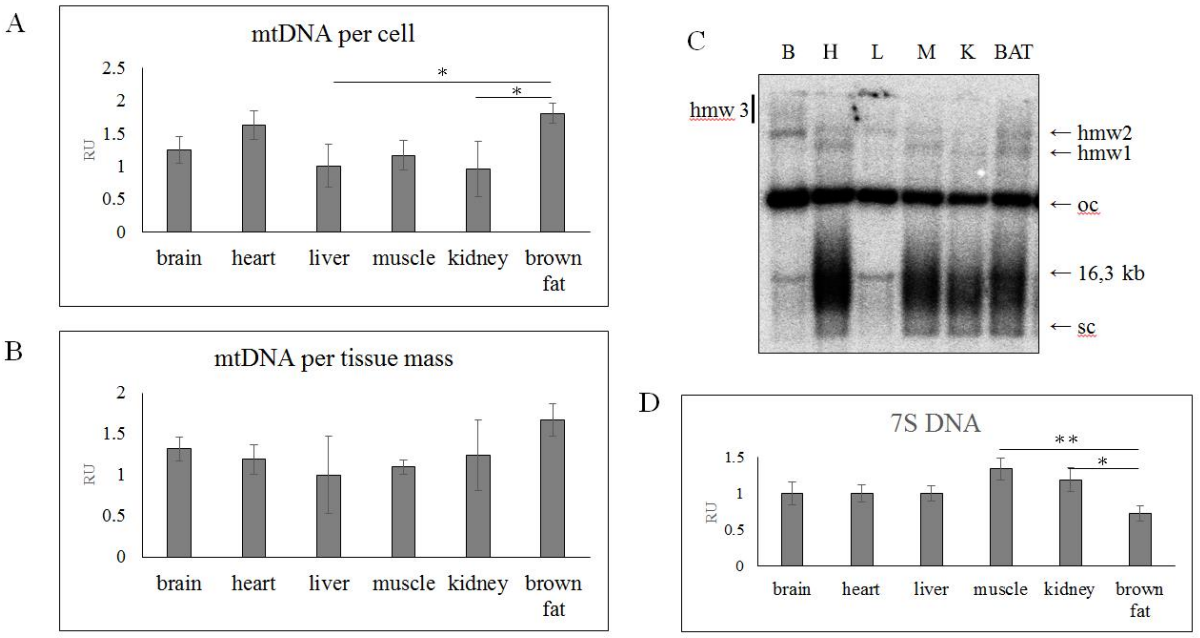

Figure 2

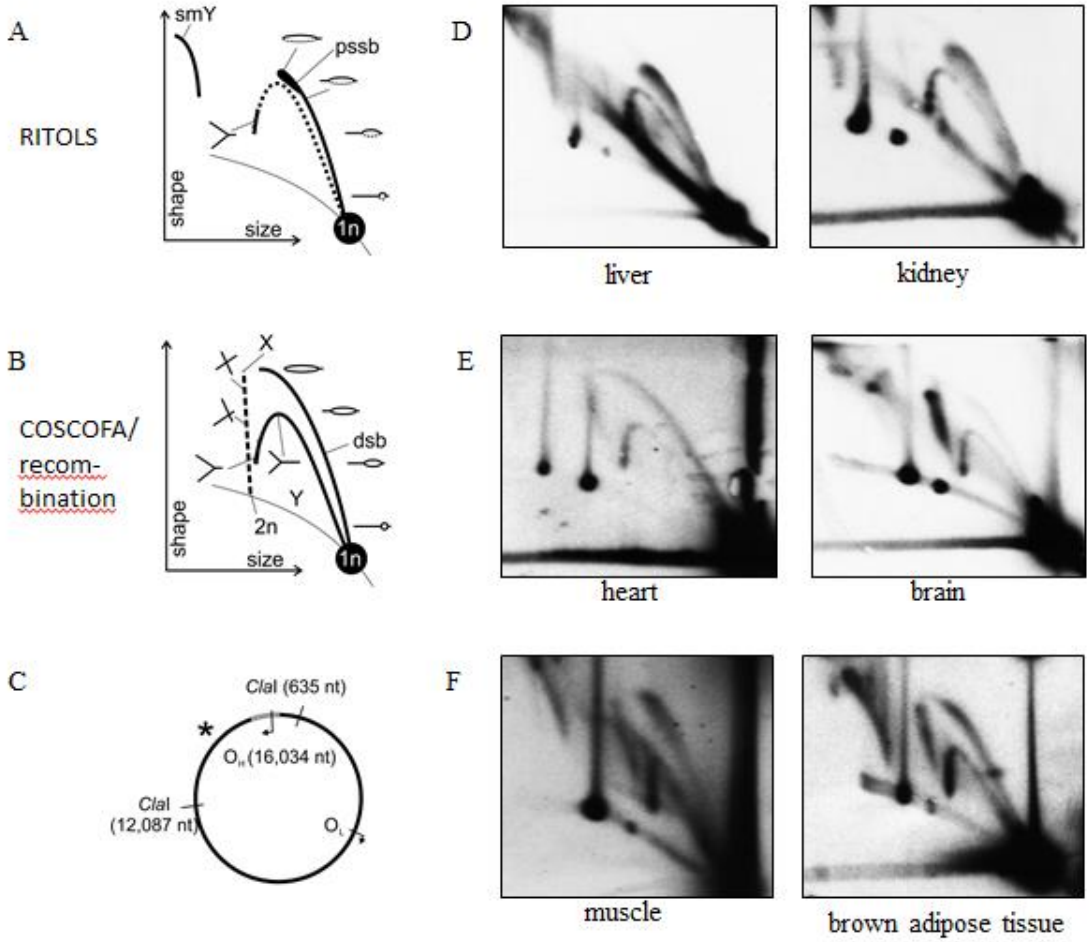

Figure 3

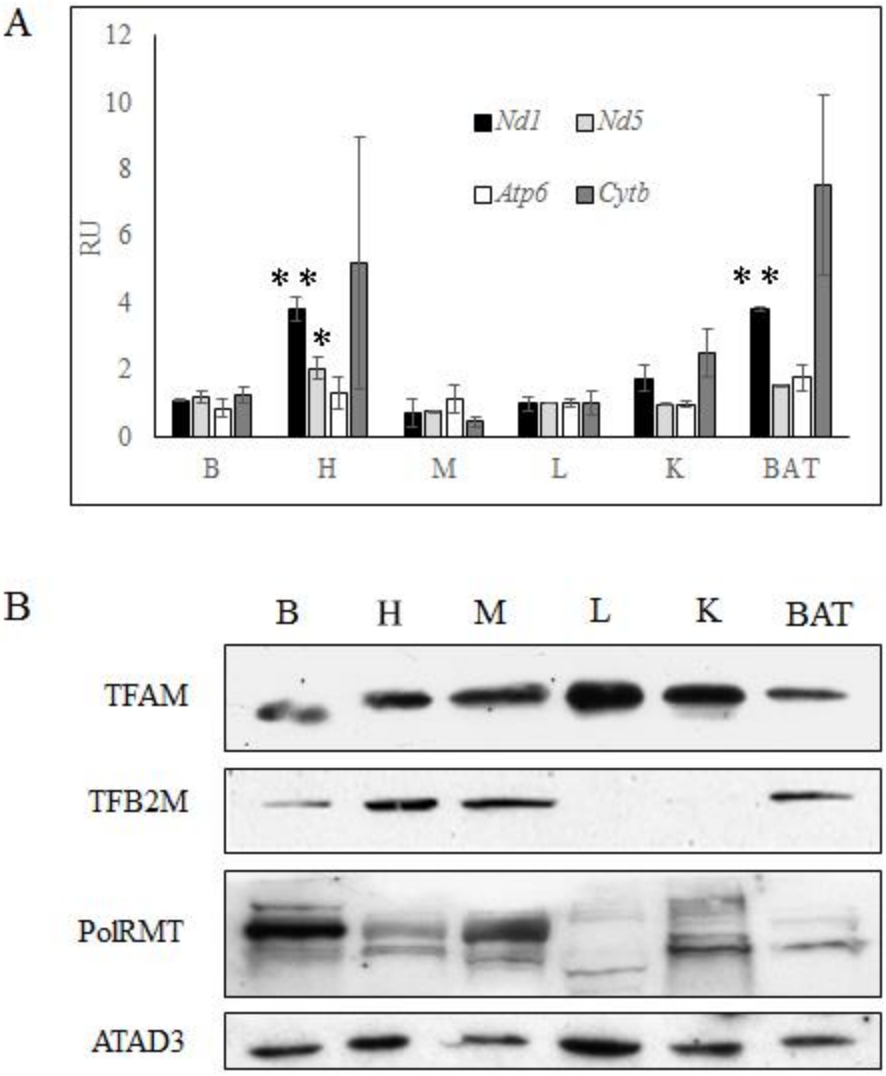

Figure 4

Highlights

- Mouse tissue employ various replication modes to maintain mitochondrial DNA
- mtDNA recombination and strand-coupled replication are prominent in tissues with high mtDNA damage